IRSTI 31.15.15 https://doi.org/10.58805/kazutb.v.3.24-514

SEMI-EMPIRICAL INVESTIGATION OF ZINC(II) SALICYLATE. COMPARISON WITH X-RAY STRUCTURE

N. Akatyev

M.Utemisov West Kazakhstan university, Uralsk, Kazakhstan,

Corresponding author: nikolay.akatyev@wku.edu.kz

Zinc salicylate dihydrate ($Zn(HSal)_2 \cdot 2H_2O$) is an organic-inorganic hybrid compound known for its wide range of applications. In this article, a detailed semiempirical study of zinc salicylate is presented, focusing on its structural, electronic, and thermodynamic properties. The PM3 method, known for its computational efficiency and reasonable accuracy, was used to model the molecular structure and compare with the experimentally obtained properties of $Zn(HSal)_2 \cdot 2H_2O$. Based on the obtained calculation results and available experimental data published in the literature, it was found that semi-empirical calculations involving the solvent effect (H_2O) agree well with data from X-ray diffraction analysis, while calculations for the gas phase do not agree with experimental data with the required accuracy. Quantum chemical descriptors such as HOMO-LUMO energies, energy gap (ΔE_{gap}), electronegativity (χ), global hardness (η), softness (σ), dipole moment (μ), electrophilic (ω) and nucleophilic (ε) indices were also calculated. The results show that the PM3 method effectively captures the essential features of zinc salicylate, including its geometry and electronic distribution. The obtained results also provide valuable insights into the semi-empirical modeling of organometallic compounds and highlight the usefulness of the PM3 method in predicting the behavior of complex molecular systems.

Keywords: PM3 calculations, zinc salicylate, semi-empirical calculations, quantum chemical descriptors.

МЫРЫШ(II) САЛИЦИЛАТЫН ЖАРТЫЛАЙ ЭМПИРИКАЛЫҚ ЗЕРТТЕУ. РЕНТГЕН ҚҰРЫЛЫМЫМЕН САЛЫСТЫРУ

Н. Акатьев

М.Өтемісов атындағы Батыс Қазақстан университеті, Орал, Қазақстан,

e-mail: nikolay.akatyev@wku.edu.kz

Мырыш салицилат дигидраты ($Zn(HSal)_2 \cdot 2H_2O$), қолдану аясының кең ауқымымен танымал органикалық - бейорганикалық гибридті қосылыс. Бұл мақалада оның құрылымдық, электронды және термодинамикалық қасиеттеріне назар аудара отырып, мырыш салицилатының егжей-тегжейлі жартылай эмпирикалық зерттеуі ұсынылған. Молекулярлық құрылымды модельдеу және $Zn(HSal)_2 \cdot 2H_2O$-ның тәжірибелік алынған қасиеттерімен салыстыру үшін өзінің есептеу тиімділігі мен ақылға қонымды дәлдігімен танымал PM3 әдісі қолданылды. Алынған есептеу нәтижелеріне және әдебиетте жарияланған қолда бар эксперименттік деректерге сүйене отырып, еріткіш әсерін (H_2O) қамтитын жартылай эмпирикалық есептеулер рентгендік дифракциялық талдау деректерімен жақсы сәйкес келеді, ал газ фазасы үшін есептеулер сәйкес келмейтіні анықталды. қажетті дәлдікпен эксперименттік деректермен. HOMO-LUMO энергиясы, энергетикалық алшақтық (ΔE_{gap}), электртерістілік (χ), ғаламдық қаттылық (η), жұмсақтық (σ), дипольдік момент (μ), электрофильдік (ω) және нуклеофильдік (ε) индекстері сияқты кванттық химиялық дескрипторлар да болды. есептелген. Нәтижелер PM3

әдісі мырыш салицилатының маңызды ерекшеліктерін, соның ішінде оның геометриясын және электрондық таралуын тиімді түрде түсіретінін көрсетеді. Алынған нәтижелер сонымен қатар металлорганикалық қосылыстардың жартылай эмпирикалық модельделуіне құнды түсініктер береді және күрделі молекулалық жүйелердің әрекетін болжауда PM3 әдісінің пайдалылығын көрсетеді.

Түйін сөздер: PM3 есептеулері, мырыш салицилаты, жартылай эмпирикалық есептеулер, квантық химиялық дескрипторлар.

ПОЛУЭМПИРИЧЕСКОЕ ИССЛЕДОВАНИЕ САЛИЦИЛАТА ЦИНКА(II). СРАВНЕНИЕ С РЕНТГЕНОВСКОЙ СТРУКТУРОЙ

Н. Акатьев

Западно-Казахстанский университет им.М.Утемисова, Уральск, Казахстан,

e-mail: nikolay.akatyev@wku.edu.kz

Дигидрат салицилата цинка ($Zn(HSal)_2 \cdot 2H_2O$)- гибридное органо-неорганическое соединение, известное своим широким спектром применения. В данной статье представлено подробное полуэмпирическое исследование салицилата цинка с упором на его структурные, электронные и термодинамические свойства. Для моделирования молекулярной структуры и сравнения с экспериментально полученными свойствами $Zn(HSal)_2 \cdot 2H_2O$ был использован метод PM3, известный своей вычислительной эффективностью и приемлемой точностью. На основании полученных расчётов и имеющихся экспериментальных данных, опубликованных в литературе, установлено, что полуэмпирические расчёты с учетом эффекта растворителя (H_2O) хорошо согласуются с данными рентгеноструктурного анализа, тогда как расчеты для газовой фазы не согласуются с экспериментальными данными с необходимой точностью. Были рассчитаны квантово-химические дескрипторы, такие как энергии ВЗМО-НВМО, энергетическая щель (ΔE_{gap}), электроотрицательность (χ), глобальная твердость (η), мягкость (σ), дипольный момент (μ), электрофильные (ω) и нуклеофильные (ε) индексы. Результаты показывают, что метод PM3 эффективно отражает основные характеристики салицилата цинка, включая его геометрию и электронное распределение. Полученные результаты также дают ценную информацию о полуэмпирическом моделировании металлоорганических соединений и подчеркивают полезность метода PM3 для прогнозирования поведения сложных молекулярных систем.

Ключевые слова: PM3 расчёты, салицилат цинка, полуэмпирические расчёты, квантово - химические дескрипторы.

Introduction. Numerous branches of chemistry place significant theoretical and practical emphasis on the structure and characteristics of transition metal salicylates. These simple organic salts of salicylic acid (*o*-hydroxybenzoic acid) have a wide range of applications because of their beneficial qualities. Compounds with carboxyl groups are intriguing from the standpoint of coordination chemistry because they can bind to metal ions as mono-, bi-, and bridging ligands.

Over the last two decades, a wide range of transition metal complexes containing salicylate and its various derivatives have been described. Das *et al.* reported a highly porous and thermally stable Co(II) salicylate metal–organic framework (MOF). Obtained material has very interesting magnetic properties, in which the magnetic moments increase with decreasing temperature [1]. A metal-containing ionic liquid (MCIL) has been also prepared in which the $[Co^{II}(Sal)_2]^{2-}$ anion is able to selectively coordinate two water molecules with a visible color change [2]. Chakraborty and Paine synthesized and structurally characterized four mononuclear cobalt-salicylate complexes

derived from N4-donor ligands. A hexameric water cluster is stabilized in the lattice of hydrated crystal complex [3]. A manganese complex with a salicylic acid residue was reported by Devereux *et al*. In the presence of imidazole, the complex powerfully catalyzes the disproportionation of hydrogen peroxide [4]. Square-planar bis(N,N-dimethylbiguanide)nickel(II) salicylate and hexakis(imidazole)nickel(II) disalicylate were also reported by Lemoine [5] and Jian [6] respectively. Copper salicylate is known as an anti-inflammatory agent [7].

Zinc is an essential trace element in the human body for activating (as a cofactor) more than 200 zinc-dependent metalloenzymes [8]. In addition, zinc is urgently needed for human health due to its critical role in growth, metabolism and wound healing [9,10]. It is the second most abundant micronutrient in the human body after iron [11]. Zinc also plays a central role in plant defense against pathogens and herbivores [12]. Nevertheless, overaccumulation of zinc leads to morphological, biochemical, and physiological disorders and can be toxic to flora, fauna and humans [13].

Zinc salicylate is interesting for its biological activity. It is known as a component of antifouling coatings and has been demonstrated by Bellotti and Romagnoli to be effective against *Artemia larvae* with lower toxicity than copper [14]. Fang compared the zinc salicylate-methylsulfonylmethane complex with zinc salicylate, sodium salicylate and zinc chloride in terms of the remodeling parameters of human airway smooth muscle cells (ASMC) [15]. In addition, zinc salicylate is described as a carbon source for templating porous carbons for supercapacitors [16]. Some other zinc salicylate-derived complexes have been studied by Brownless [17] and Chooset [18].

In contemporary theoretical science, the quantum chemical approach is used to extend on experimental investigations and to find appropriate theoretical parameters to describe or interpret the experimental results. On the other hand, computational methods make it possible to predict the variety of practically important properties of substances and complex systems based on electronic density, charge distribution or other descriptors. Techniques based on density functional theory (DFT) have long been used to study the electronic structure of transition metal compounds. However, this approach is still extremely computationally intensive and may not be practical for many systems of interest [19]. Semi-empirical methods are much faster and therefore have great potential to produce acceptable results. Higher speed comes at the expense of the approximations made in evaluating the integrals describing the interactions between nuclei and some electron integrals of the electrons (considered negligible) are ignored while others are estimated from experiments [20]. In our research, we used the semi-empirical quantum chemical method PM3 to investigate the properties of the zinc (II) salicylate dihydrate $Zn(HSal)_2 \cdot 2H_2O$.

Materials and methods. Like other semi-empirical methods, PM3 is a self-consistent-field (SCF) method. All calculated integrals are evaluated using approximate values. Semiempirical calculations of transition metal complexes are orders of magnitude cheaper than their *ab initio* and most DFT counterparts and are extremely productive in the field of theoretical organic chemistry. However, the parameterization of these methods for transition metal systems is not trivial. Nevertheless, some attempts have been made to introduce *d*-orbitals into traditional semi-empirical methods. The PM3 method has a range of parameters for transition metals [21]. It is the most applicable semi-empirical method for calculating zinc compounds with Zn^{+2}. AM1 produces errors 30% larger than PM3. Owing to errors in its original parametrization, MNDO/d is not appropriate for use in computations [22].

All quantum chemical calculations were performed on a desktop PC with Windows 11, a 12^{th} generation Intel(R) Core (TM) i7-12700H 2.30 GHz, 16GB RAM) with GAMESS software [23]. The programs Avogadro [24] and Jmol [25] were used to prepare the input file and visualize the results respectively. Initially, full geometry optimization was achieved using the Molecular Mechanics (MM+) force field in the gas phase. The results from MM+ were further selected as input and re-optimized using semi-empirical

PM3 [26] to obtain the equilibrium geometry with a root mean square (RMS) gradient of 0.001 kcal/Å·mol. This calculation method requires little computational effort and provides good agreement with the experiment. Semiempirical methods can be applied to calculations of much larger systems than classical *ab initio* or DFT methods, sometimes achieving accuracy comparable to more advanced levels of theory [27]. Method based on neglecting the integral approximation of differential diatomic overlap, representing an excellent compromise between completeness and economy. The molecular geometry was fully optimized using the analytical gradient method implemented in the program package without any limitations. The computational study was carried out in the gas and solution phases. Water was used to incorporate the solvent effect. To better approximate the experimental results in the solution phase, Tomasi's Polarized Continuum Model PCM was used.

The following quantum chemical indices, describing global reactivity were considered: the energy of the highest occupied molecular orbital (E_{HOMO}), the energy of the lowest unoccupied molecular orbital (E_{LUMO}), energy gap (ΔE_{gap}), the ionization potential (IP), the electron affinity (EA), electronegativity (χ), global hardness (η), softness (σ), dipole moment (μ), electrophilic (ω) and nucleophilic (ε) indexes. They were calculated using formulas 1-8:

$$\Delta E_{gap} = E_{LUMO} - E_{HOMO} \quad (1)$$

$$IP = -E_{HOMO} \quad (2)$$

$$EA = E_{LUMO} \quad (3)$$

$$X = \frac{I + A}{2} \quad (4)$$

$$\eta = \frac{I - A}{2} \quad (5)$$

$$\sigma = \frac{1}{\eta} \quad (6)$$

$$\omega = \frac{X^2}{2\eta} \quad (7)$$

$$\varepsilon = \frac{1}{\omega} \quad (8)$$

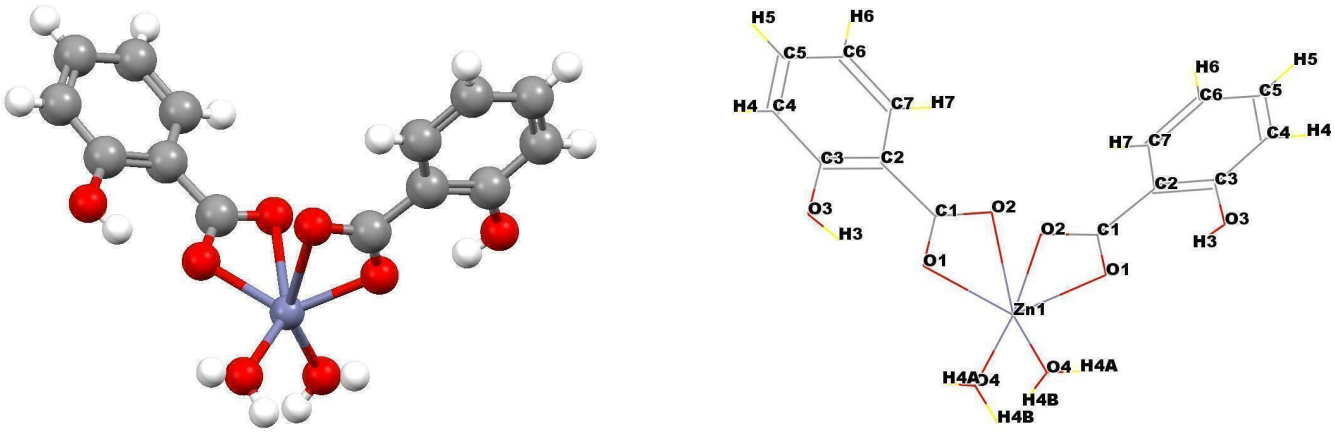

Figure 1 - Structural formula of the $Zn(HSal)_2 \cdot 2H_2O$ molecule obtained with X-ray diffraction by Gusev *et al.*

According to the Koopman's theorem, the HOMO energy is related to IP while the LUMO energy is related to EA (Eq. 2, 3). Electronegativity (χ) and global hardness (η) were evaluated based on the finite difference approximation as linear combinations of the calculated IP and EA [28] (Eq. 4, 5). The global softness (σ) is the reciprocal of the global hardness [29] (Eq. 6).

The global electrophilicity index (ω) describes the stabilization of a molecule after the acquisition of an additional number of electrons (Eq. 7). The nucleophilicity index (ε) is the reciprocal of the global electrophilicity index (Eq. 8).

Results and discussion. The aim of this research is to study $Zn(HSal)_2 \cdot 2H_2O$ in the gas and aqueous phases from a structural and energetic perspective using quantum chemical descriptors calculated using the semi-empirical PM3 method. Another aim is to compare the calculated geometry with the available detailed X-ray structural data obtained by Gusev *et al* [30]. The molecular structure is close to $Zn(HSal)_2 \cdot 2H_2O$ (Figure 1). The substance belongs to the space group C_2 and the monoclinic crystal system.

The crystal structure of zinc (II) salicylate dihydrate was first described by Klug [31]. The thermal behavior of zinc salicylate and 5-chlorosalicylate complexes with bioactive ligands was studied by Chomič *et al* [32,33]. The stability constant of zinc (II) salicylate was determined by Singh [34].

Bond length. As part of our investigation, we first presented the PM3-optimized geometry parameters (bond length and angle) in the gas and aqueous phases in comparison to available X-ray analysis data. The calculated and experimental values of the bond lengths are listed in Table 1. The list of atoms corresponds to Figure 1.

A comparison of the calculated bond lengths of zinc salicylate with X-ray structural data shows that they agree well in the case of the aqueous phase. For example, the calculated length of the Zn1-O1 bond is 1.9897Å while the experimental value is 1.9928Å. These values lie within acceptable deviations. Bond length values calculated for the gas phase are less consistent with experimental results. In addition, the calculated bond lengths of the zinc salicylate molecule in the gas phase are slightly longer than in aqueous phase. An exception are the Zn(1)-O(4) coordination bonds and the O-H-bond in coordinated water molecules, whose lengths were significantly longer for the gas phase.

The lengths of the C=C bonds in the benzene ring are typical for aromatic compounds. The calculated length also agrees well with the reference data.

Bond angles. Experimental and calculated values of the bond angles are listed in Table 2.

A comparison of the results of the PM3 zinc salicylate bond angle calculations show the same trend as the results of the bond length calculations. The angle values obtained for the aqueous phase agree well with the X-ray diffraction results. The calculation for the gas phase shows a significantly lower correlation to experimental data. It can be clearly concluded that the best results for calculating the geometry of such molecules can be obtained for the solution phase. In this case, gas phase calculations are performed with significant errors.

Таблица 1 - Comparison between experimental X-ray and PM3 calculated bond lengths (Å) of $Zn(HSal)_2 \cdot 2H_2O$ for the gas and aqueous phases.

Atom 1	Atom 2	Bond length, Å		
		XRD data	Gas phase	Aqueous phase
Zn1	O1	1.9928	2.1156	1.9897
Zn1	O2	2.5679	2.3277	2.5815
Zn1	O4	1.9857	2.3194	2.0294
Zn1	O1	1.9928	2.1156	1.9897
Zn1	O2	2.5679	2.2659	2.5815
Zn1	O4	1.9857	2.3042	2.0294
O1	C1	1.2830	1.3328	1.2651
O2	C1	1.2533	1.2584	1.2312

Continued on next page

Atom 1	Atom 2	Bond length, Å		
		XRD data	Gas phase	Aqueous phase
O3	C3	1.3641	1.3760	1.3874
O3	H3	0.7692	0.9580	0.7716
O4	H4A	0.6499	0.9452	0.6498
O4	H4B	0.8521	0.9413	0.8136
C1	C2	1.4796	1.4894	1.4682
C7	H7	0.9306	1.1000	0.9077
C7	C2	1.4039	1.3953	1.4079
C7	C6	1.3806	1.3940	1.4053
C3	C2	1.4065	1.3394	1.3907
C3	C4	1.3874	1.4232	1.3667
C5	H5	0.9303	1.1108	0.9208
C5	C6	1.3964	1.3451	1.3966
C5	C4	1.3860	1.3396	1.3737
C6	H6	0.9305	1.0886	0.8965
C4	H4	0.9291	1.1186	0.8952
O1	C1	1.2830	1.3328	1.2651
O2	C1	1.2532	1.2584	1.2312
O3	C3	1.3641	1.3760	1.3874
O3	H3	0.7691	0.9580	0.7716
O4	H4A	0.6499	0.9452	0.6498
O4	H4B	0.8521	0.9413	0.8136
C1	C2	1.4796	1.4894	1.4682
C7	H7	0.9306	1.1000	0.9077
C7	C2	1.4039	1.3953	1.4079
C7	C6	1.3806	1.3940	1.4053
C3	C2	1.4065	1.3394	1.3907
C3	C4	1.3874	1.4232	1.3667
C5	H5	0.9303	1.1108	0.9208
C5	C6	1.3964	1.3451	1.3966
C5	C4	1.3861	1.3396	1.3737
C6	H6	0.9305	1.0886	0.8965
C4	H4	0.9292	1.1186	0.8952

Таблица 2 - Table 2 - Bond angle properties of $Zn(HSal)_2 \cdot 2H_2O$ obtained from XRD and calculated using the PM3 method.

Atom 1*	Atom 2*	Atom 3*	Bond angle (deg)		
			XRD data	Gas phase	Aqueous phase
O1	Zn1	O2	56.03	57.27	55.07
O1	Zn1	O4	120.11	112.40	119.68
O1	Zn1	O1	128.18	145.40	127.48
O1	Zn1	O2	86.98	99.58	85.12
O1	Zn1	O4	92.86	91.74	90.46

(continued)

Atom 1*	Atom 2*	Atom 3*	Bond angle (deg)		
			XRD data	Gas phase	Aqueous phase
O2	Zn1	O4	91.72	90.81	90.85
O2	Zn1	O1	86.98	99.90	85.12
O2	Zn1	O2	91.21	99.56	90.54
O2	Zn1	O4	148.53	147.68	147.65
O4	Zn1	O1	92.86	88.28	90.46
O4	Zn1	O2	148.53	143.73	147.65
O4	Zn1	O4	101.74	91.92	101.00
O1	Zn1	O2	56.03	57.27	55.07
O1	Zn1	O4	120.11	114.71	119.68
O2	Zn1	O4	91.72	94.38	90.85
Zn1	O1	C1	104.47	98.21	104.94
Zn1	O2	C1	78.62	91.07	77.49
C3	O3	H3	106.76	107.91	104.75
Zn1	O4	H4A	114.69	100.15	111.15
Zn1	O4	H4B	120.35	102.46	120.99
H4A	O4	H4B	122.19	101.98	121.35
O1	C1	O2	120.46	111.12	121.99
O1	C1	C2	118.01	121.43	117.24
O2	C1	C2	121.51	121.71	120.72
H7	C7	C2	119.30	119.59	118.93
H7	C7	C6	119.30	120.93	119.60
C2	C7	C6	121.40	120.25	119.55
O3	C3	C2	121.63	123.88	121.59
O3	C3	C4	117.81	128.18	117.40
C2	C3	C4	120.56	120.39	120.88
C1	C2	C7	120.06	120.34	120.28
C1	C2	C3	121.64	120.60	121.20
C7	C2	C3	118.23	119.44	118.47
H5	C5	C6	119.70	119.83	117.08
H5	C5	C4	119.72	119.37	119.23
C6	C5	C4	120.58	116.83	121.68
C7	C6	C5	119.26	120.35	118.71
C7	C6	H6	120.34	119.77	119.83
C5	C6	H6	120.40	116.49	120.69
C3	C4	C5	119.96	129.69	118.94
C3	C4	H4	120.00	119.77	120.06
C5	C4	H4	120.04	114.33	120.96
Zn1	O1	C1	104.47	96.94	104.96
Zn1	O2	C1	78.62	98.38	77.49
C3	O3	H3	106.77	106.71	104.75
Zn1	O4	H4A	114.69	102.46	111.15
Zn1	O4	H4B	120.34	100.65	120.99

(continued)

Atom 1*	Atom 2*	Atom 3*	Bond angle (deg)		
			XRD data	Gas phase	Aqueous phase
H4A	O4	H4B	122.20	108.95	121.35
O1	C1	O2	120.46	111.12	121.99
O1	C1	C2	118.01	121.30	117.24
O2	C1	C2	121.51	121.71	120.72
H7	C7	C2	119.30	119.41	118.93
H7	C7	C6	119.30	122.79	119.60
C2	C7	C6	121.40	120.46	119.55
O3	C3	C2	121.63	124.63	121.59
O3	C3	C4	117.81	128.18	117.40
C2	C3	C4	120.56	120.21	120.88
C1	C2	C7	120.06	120.55	120.28
C1	C2	C3	121.64	120.29	121.20
C7	C2	C3	118.23	119.44	118.47
H5	C5	C6	119.70	119.56	117.08
H5	C5	C4	119.72	123.61	119.23
C6	C5	C4	120.57	116.83	121.68
C7	C6	C5	119.26	120.37	118.71
C7	C6	H6	120.34	119.72	119.83
C5	C6	H6	120.39	121.05	120.69
C3	C4	C5	119.96	119.70	118.94
C3	C4	H4	120.00	119.43	120.06
C5	C4	H4	120.04	121.11	120.96
* - *numbering of atoms is in accordance with Fig.1.*					

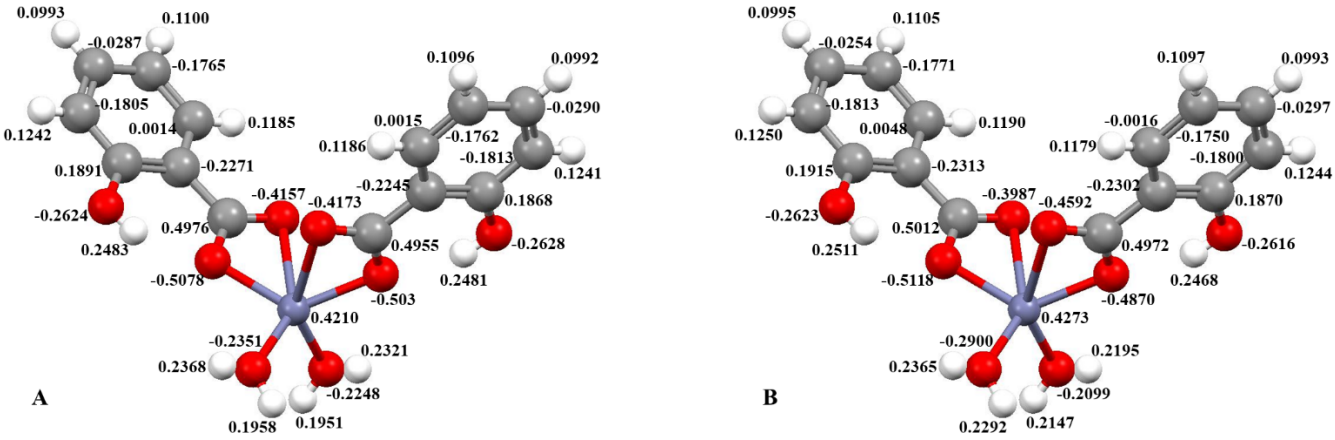

Figure 2 - PM3 Mulliken charges population for the calculated $Zn(HSal)_2 \cdot 2H_2O$ molecule in gas (A) and aqueous (B) phase.

Mulliken charges population analysis. The local reactivity of zinc salicylate was studied using Mulliken charge population analysis, which provides an indication of the reactive (nucleophilic and electrophilic) centers of molecules. Therefore, the regions of the molecule with high electronic

charge are chemically softer than the regions with low electronic charge, so electron density plays an important role in chemical reactivity calculations. The results of the Mulliken atomic charge calculation are shown in Figure 2.

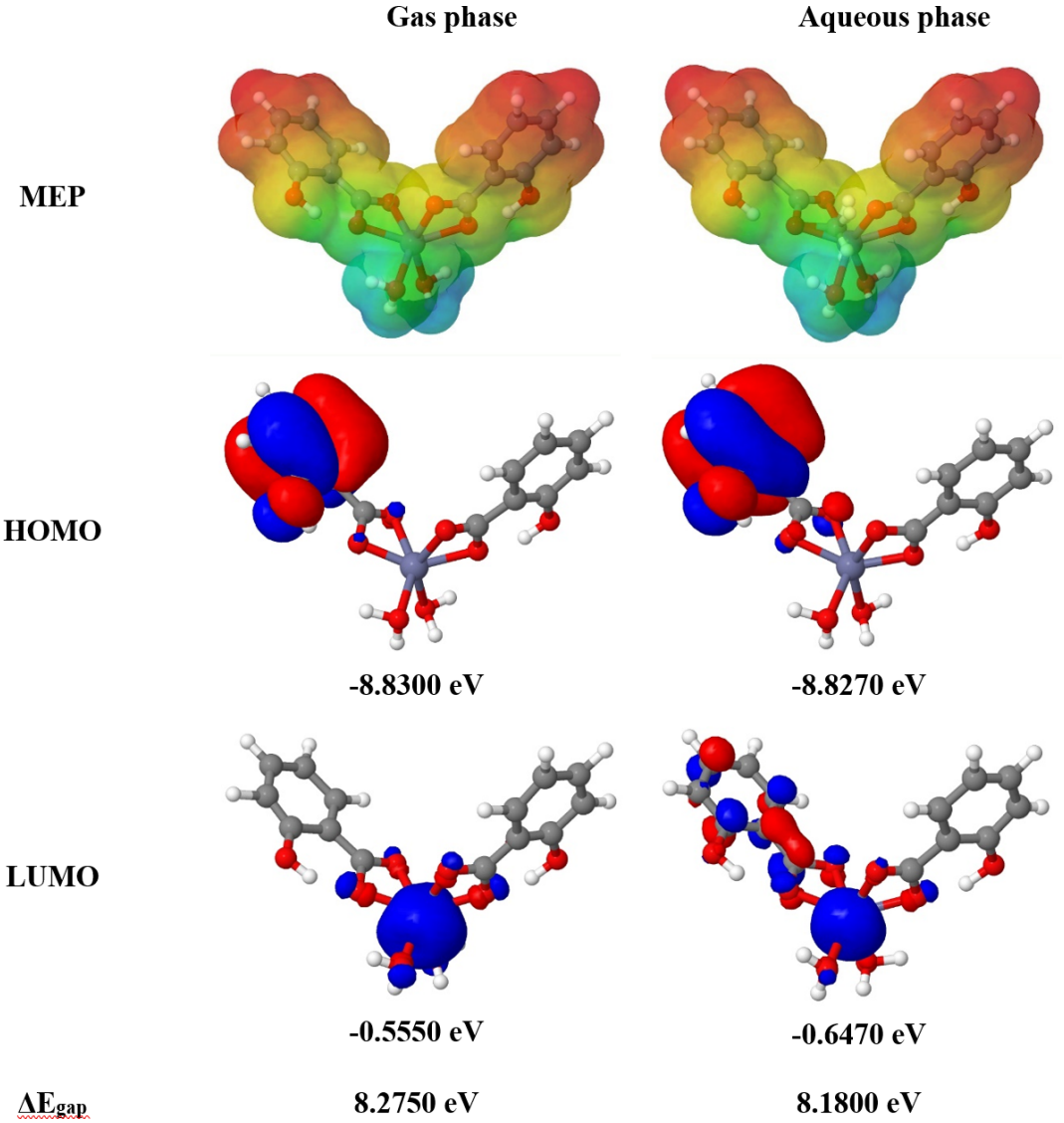

Figure 3 - The molecular electrostatic potential (MEP) and frontier molecular orbitals (HOMO-LUMO) density distribution of the $Zn(HSal)_2 \cdot 2H_2O$ calculated with PM3 for gas and aqueous phases.

The place for a nucleophilic attack is where the value of the positive charge is maximum. The location of electrophilic attack is in turn controlled by the negative charge value. Mulliken charge population analysis shows that the zinc atoms in both the gas and aqueous phases have the maximum positive charge. The most negative charges are on the oxygen atoms of the carboxyl groups. Consequently, the oxygen atoms of the carboxyl groups are most susceptible to electrophilic attack. The presence of water leads to a slight shift in the electron density towards the oxygen atoms of the carboxyl groups, which becomes more negative.

Frontier molecular orbitals (FMO). Frontier orbital theory is very useful for determining the main properties of molecules. The positions of the highest occupied molecular orbital (HOMO) and the lowest unoccupied molecular orbital (LUMO)

are molecular parameters that are directly related to the electron and hole transport properties of the substance. The energy gap value (ΔE_{gap}) is the difference between HOMO-LUMO and is used as a significant descriptor of molecular stability. The most stable molecule has a low ΔE_{gap}.

The molecular electrostatic potential (MEP), frontier molecular orbitals energies and ΔE_{gap} calculated for $Zn(HSal)_2 \cdot 2H_2O$ are shown in Figure 3.

The positively charged lobe is indicated by the blue color, and the negatively charged lobe is indicated by the red color.

E_{HOMO} describes the electron donating ability of the molecule. Conversely, E_{LUMO} describes the ability of the molecule to accept electrons. The lower the LUMO value, the higher the ability of the compound to accept electrons. The HOMOs of $Zn(HSal)_2 \cdot 2H_2O$ are mainly located at the oxygen atoms of the -OH-group in the ortho-position. On the other hand, the LUMOs are mainly located on the zinc atoms and oxygen atoms of the carboxyl units. The presence of water as a high dielectric constant model solvent results in a slight decrease in the LUMO energy (around 0.095 eV) and a non-significant decrease in the HOMO energy.

Negative values for E_{HOMO} and E_{LUMO} indicate the presence of additional electron pairs in both the upper and lower molecular orbitals. This means that zinc salicylate should act as an electron donor in chemical transformations. A low negative LUMO value (near zero) indicates that zinc salicylate is a weak electrophile.

The gap energy (ΔE_{gap}, Eq.1.) between the frontier orbitals is usually of great importance in describing static molecular reactivity. Large energy gap values mean high electronic stability and therefore low reactivity. In the gas phase, zinc salicylate has a higher ΔE_{gap} value than in solution (8.275 eV and 8.180 eV respectively). Therefore, zinc salicylate is more stable in the gas phase than in solution. Under the influence of polar water molecules, zinc salicylate becomes unstable as it dissolves and dissociates into ions.

Quantum chemical descriptors. In accordance with the relationship of HOMO-LUMO energy values, the reactivity descriptors of the $Zn(HSal)_2 \cdot 2H_2O$ molecule were calculated using formulas 2-8 in gas and aqueous phases. The calculation results obtained are shown in Table 3.

The heat of formation value provides a quantitative estimate of the energy required to destroy the molecule. The negative value of the heat of formation indicates the high stability of the substance both in the gas phase (-1079.97 kJ/mol) and in the aqueous phase (-1102.97 kJ/mol). A more negative value indicates greater stability of zinc salicylate in the aqueous phase. PM3 predicts these values for a standard thermodynamic temperature of 298.15 K.

Table 3 - Quantum chemical descriptors of the $Zn(HSal)_2 \cdot 2H_2O$ molecule calculated using the PM3 method in the gas and aqueous phase.

Descriptor	Gas phase	Aqueous phase
Heat of formation (ΔHf), kJ/mol	-1079.97	-1102.20
Dipole moment (μ), D	4.9320	3.9620
Ionization energy (IP), eV	8.8300	8.8270
Electron affinity (EA), eV	0.5550	0.6470
Electronegativity (χ), eV	4.6925	4.7370
Chemical hardness (η), eV	4.1375	4.0900
Chemical softness (σ), eV	0.2417	0.2445
Electrophilicity index (ω), eV	2.6610	2.7432
Nucleophilicity index (ε), eV	0.3758	0.3645

Comparison of the calculated dipole moment (μ) of zinc salicylate (4,9320 D gas, 3.9620 D aqueous) with the dipole moments of water (1.83 D) and alcohols (CH_3OH 1.69 D, C_2H_5OH 1.66 D) shows its good solubility in polar solvents, especially in water. Dipole moment values also show that zinc salicylate readily dissolves in aprotic polar solvents such as dimethylacetamide (3.72 D), N,N-dimethylformamide (3.86 D), N-methylpyrrolidone (4.09 D), dimethyl sulfoxide (4.1 D) and propylene carbonate (4.94 D). Zinc salicylate should be insoluble in non-polar solvents.

Electronegativity indicates the molecular ability to accept electrons. The structure obtained in the aqueous phase becomes more electronegative than in the gas phase. Value of global hardness (η) based on 4.137 eV and 4.09 eV for the gas and aqueous phases, respectively. This means that zinc salicylate is a hard reagent in both phases and a better electrophile in the aqueous phase.

The global softness (σ) is the reciprocal of the global hardness [35]. Both are related to the principle of hard and soft acid and base (HSAB) and are very useful in explaining various experimental observations. These parameters characterize the molecule as a whole. Softness is an important property for measuring the molecular stability and reactivity. The calculated softness value for zinc salicylate is higher in aqueous than in the gas phase.

The global electrophilicity index (ω) introduced by Parr [36,37], is a measure of energy stabilization after a molecule has acquired an additional amount of electrons. As shown in Table 3, zinc salicylate has the highest value of electrophilicity index in the aqueous phase. Therefore, zinc salicylate is chemically more reactive in the gas phase.

Conclusion. In this research, $Zn(HSal)_2 \cdot 2H_2O$ was studied using the semi-empirical PM3 computational approach. The calculations were carried out for the gas and aqueous phases. The calculations performed in the present study predict that the calculated geometric parameters are close to those from X-ray studies. A comparison of the available X-ray crystallographic data and the theoretical results obtained shows that there is a large correlation. The best agreement was found for the aqueous phase calculations. PM3 calculation of the geometry of zinc salicylate dihydrate performs quite well in terms of both bond distances and bond angles. The agreement between calculated and experimental data is satisfactory, especially in the case of the aqueous phase calculation. Therefore, this approach is promising for application to such systems.

References

1. Das S. K. et al. Highly porous Co (II)-salicylate metal–organic framework: synthesis, characterization and magnetic properties //Dalton Transactions. – 2011. – Vol. 40 (12) – P. 2932-2939.

https://doi.org/10.1039/C0DT01483D

2. Kohno Y. *et al.* A cobalt (II) bis (salicylate)-based ionic liquid that shows thermoresponsive and selective water coordination //Chemical Communications. – 2014. – Vol. 50 (50) – P. 6633-6636.

https://doi:10.1039/c4cc01023j

3. Chakraborty B., Paine T. K. Synthesis and characterization of cobalt (II)–salicylate complexes derived from N4-donor ligands: Stabilization of a hexameric water cluster in the lattice host of a cobalt (III)–salicylate complex //Inorganica Chimica Acta. – 2011. – Vol. 378 (1) – P. 231-238.

https://doi.org/10.1016/j.ica.2011.09.008

4. Devereux M. *et al.* Manganese (II) salicylate complexes as H_2O_2 disproportionation catalysts: X-ray crystal structure of $[Mn(Hsal)_2 (bipy)]\cdot H_2O$ (H_2sal= salicylic acid, bipy= 2,2′-bipyridine) //Polyhedron. – 1996. – Vol. 15 (12) – P. 2029-2033. https://doi.org/10.1016/0277-5387(95)00452-1

5. Lemoine P. *et al.* Crystal structure of bis (N,N-dimethylbiguanide) nickel (II) salicylate, $C_{22}H_{32}N_{10}NiO_6$ //Zeitschrift für Kristallographie-New Crystal Structures. – 1999. – Vol. 214 (3) – P. 369-370.

https://doi.org/10.1515/ncrs-1999-0337

6. Jian F. *et al*. Structure of hexakis (imidazole) nickel (II) disalicylate,$[Ni(Im)_6](Sal)_2$ //Journal of chemical crystallography. – 1999. – Vol. 29. – P. 359-363. https://doi.org/10.1023/A:1009542422416

7. Auer D. E., Ng J. C., Seawright A. A. Copper salicylate and copper phenylbutazone as topically applied anti-inflammatory agents in the rat and horse //Journal of Veterinary Pharmacology and Therapeutics. – 1990. – Vol (1) – P. 67-75. https://doi.org/10.1111/j.1365-2885.1990.tb00749.x

8. Ünaleroğlu C., Zümreoğlu-Karan B., Mert Y. Zinc ascorbate: a combined experimental and computational study for structure elucidation //Journal of molecular structure. – 2002. – Vol. 605 (2-3) – P. 227-233. https://doi.org/10.1016/S0022-2860(01)00765-7

9. Lansdown A. B. G. *et al*. Zinc in wound healing: theoretical, experimental, and clinical aspects //Wound repair and regeneration. – 2007. – Vol. 15 (1) – P. 2-16. https://doi.org/10.1111/j.1524-475X.2006.00179.x

10. Lin P. H. *et al.* Zinc in wound healing modulation //Nutrients. – 2017. – Vol. 10 (1) – P. 16.

https://doi.org/10.3390/nu10010016

11. Scrimshaw N. S., Young V. R. The requirements of human nutrition //Scientific American. – 1976. – Vol. 235 (3) – P. 50-65. http://www.jstor.org/stable/24950435

12. Cabot C. *et al*. A role for zinc in plant defense against pathogens and herbivores //Frontiers in plant science. – 2019. – Vol. 10. – P. 1171. https://doi.org/10.3389/fpls.2019.01171

13. Balafrej H. et al. Zinc hyperaccumulation in plants: A review //Plants. – 2020. – Vol. 9 (5) – P. 562. https://doi.org/10.3390/plants9050562

14. Bellotti N., Romagnoli R. Assessment of zinc salicylate as antifouling product for marine coatings //Industrial & Engineering Chemistry Research. – 2014. – Vol. 53 (38) – P. 14559-14564.

https://doi.org/10.1021/ie5015734

15. Fang L. *et al*. Zinc salicylate reduces airway smooth muscle cells remodelling by blocking mTOR and activating $p21^{(Waf1/Cip1)}$ //The Journal of Nutritional Biochemistry. – 2021. – Vol. 89. – P. 108563. https://doi.org/10.1016/j.jnutbio.2020.108563

16. Zhang Z. J. et al. Conversion of a zinc salicylate complex into porous carbons through a template carbonization process as a superior electrode material for supercapacitors //RSC advance. – 2014. – Vol. 4 (13) – P. 6664-6671. https://doi.org/10.1039/C3RA44981E

17. Brownless N. J., Edwards D. A., Mahon M. F. Some complexes derived from zinc salicylate or 3, 5-di-tert-butylsalicylate. The crystal structure of (2,2′-bipyridyl)(methanol)(O-salicylato)(O,O′-salicylato) zinc //Inorganica chimica acta. – 1999. – Vol. 287 (1) – P. 89-94. https://doi.org/10.1016/S0020-1693(98)00421-6

18. Chooset S. *et al*. Synthesis, crystal structure, luminescent properties and antibacterial activities of zinc complexes with bipyridyl and salicylate ligands //Inorganica Chimica Acta. – 2018. – Vol. 471. – P. 493-501. https://doi.org/10.1016/j.ica.2017.11.053Get rights and content

19. Mohr M. *et al*. The use of methods involving semi-empirical molecular orbital theory to study the structure and reactivity of transition metal complexes //Faraday Discussions. – 2003. – Vol. 124. – P. 413-428. https://doi.org/10.1039/B211791F

20. Cundari T. R., Deng J. PM3 (tm) Analysis of Transition-Metal Complexes //Journal of chemical information and computer sciences. – 1999. – Vol. 39 (2) – P. 376-381. https://doi.org/10.1021/ci980145d

21. Bosque R., Maseras F. Performance of the semiempirical PM3 (tm) method in the geometry optimization of transition metal complexes //Journal of Computational Chemistry. – 2000. – Vol. 21 (7) – P. 562-571.

https://doi.org/10.1002/(SICI)1096-987X(200005)21:7<562::AID-JCC5>3.0.CO;2-0

22. Bräuer M. *et al*. Evaluation of the accuracy of PM3, AM1 and MNDO/d as applied to zinc compounds //Journal of Molecular Structure: THEOCHEM. – 2000. – Vol. 505 (1-3) – P. 289-301.

https://doi.org/10.1016/S0166-1280(99)00401-7

23. Schmidt M. W. *et al*. General atomic and molecular electronic structure system //Journal of computational chemistry. – 1993. – Vol. 14 (11) – P. 1347-1363. https://doi.org/10.1002/jcc.540141112

24. Hanwell M. D. *et al.* Avogadro: an advanced semantic chemical editor, visualization, and analysis platform //Journal of cheminformatics. – 2012. – Vol. 4. – P. 1-17. https://doi.org/10.1186/1758-2946-4-17

25. Jmol: an open-source Java viewer for chemical structures in 3D [Electronic source]. Available at: http://www.jmol.org.

26. Stewart J. J. P. Optimization of parameters for semiempirical methods II. Applications //Journal of computational chemistry. – 1989. – Vol. 10 (2) – P. 221-264. https://doi.org/10.1002/jcc.540100209

27. Pinheiro P. S. M. *et al*. Modeling zinc-oxygen coordination in histone deacetylase: a comparison of semiempirical methods performance //International Journal of Quantum Chemistry. – 2018. – Vol. 118 (21) – P. e25720. https://doi.org/10.1002/qua.25720

28. Zhan C. G., Nichols J. A., Dixon D. A. Ionization potential, electron affinity, electronegativity, hardness, and electron excitation energy: molecular properties from density functional theory orbital energies //The Journal of Physical Chemistry A. – 2003. – Vol. 107 (20) – P. 4184-4195. https://doi.org/10.1021/jp0225774

29. El Mehdi B. *et al*. Synthesis and comparative study of the inhibitive effect of some new triazole derivatives towards corrosion of mild steel in hydrochloric acid solution //Materials Chemistry and Physics. – 2003. – Vol. 77 (2) – P. 489-496. https://doi.org/10.1016/S0254-0584(02)00085-8

30. Gusev A. *et al*. Mn (II), Co (II), Ni (II) and Zn salicylates: Synthesis, structure and biological properties studies //Inorganica Chimica Acta. – 2021. – Vol. 528. – P. 120606. https://doi.org/10.1016/j.ica.2021.120606

31. Klug H. P., Alexander L. E., Sumner G. G. The crystal structure of zinc salicylate dihydrate //Acta Crystallographica. – 1958. – Vol. 11 (1) – P. 41-46. https://doi.org/10.1107/S0365110X58000086

32. Chomič J. *et al*. Thermal study of zinc (II) salicylate complex compounds with bioactive ligands //Journal of thermal analysis and calorimetry. – 2004. – Vol. 76. – P. 33-41.

https://doi.org/10.1023/B:JTAN.0000027800.14514.c2

33. Györyovő K., Chomič J., Kovőčovő J. Thermal behaviour of zinc (II) 5-chlorosalicylate complex compounds //Journal of thermal analysis and calorimetry. – 2005. – Vol. 80. – P. 375-380.

https://doi.org/10.1007/s10973-005-0663-0

34. Singh R. K. P. *et al*. Stability constants of salicylate of zinc (II), cobalt (II), uranyl (II) and thorium (IV) by paper electrophoresis //Zeitschrift für Physikalische Chemie. – 1983. – Vol. 264 (1) – P. 464-468. https://doi.org/10.1515/zpch-1983-26457

35. Pearson R. G. Absolute electronegativity and hardness: application to inorganic chemistry //Inorganic chemistry. – 1988. – Vol. 27 (4) – P. 734-740. https://doi.org/10.1021/ic00277a030

36. Parr R. G., Pearson R. G. Absolute hardness: companion parameter to absolute electronegativity //Journal of the American chemical society. – 1983. – Vol. 105 (26) – P. 7512-7516.

https://doi.org/10.1021/ja00364a005

37. Parr R. G., Szentpály L., Liu S. Electrophilicity index //Journal of the American Chemical Society. – 1999. – Vol. 121 (9) – P. 1922-1924.

https://doi.org/10.1021/ja983494x

Information about the authors

Akatyev N. V. - Candidate of Chemical Sciences, senior lecturer, M. Utemisov West Kazakhstan University, Uralsk, Kazakhstan, e-mail:nikolay.akatyev@wku.edu.kz

Сведения об авторе

Акатьев Н. В. - кандидат химических наук, старший преподаватель, Западно-Казахстанский университет им. М.Утемисова, Уральск, Казахстан, e-mail:nikolay.akatyev@wku.edu.kz